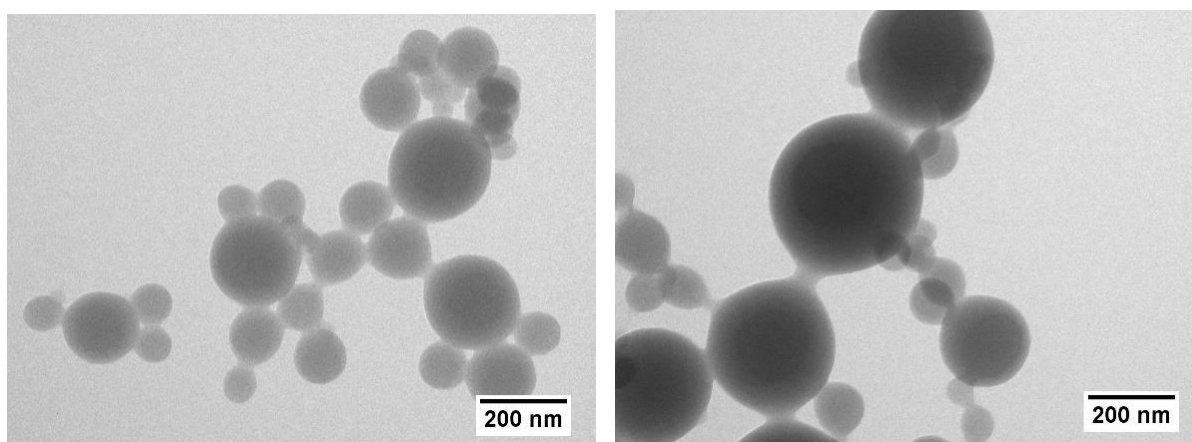


## The impact of templating and macropores in hard carbons on their properties as negative electrode materials in sodium-ion batteries

### Supporting Information

Sofiia Prykhodska<sup>a</sup>, Konstantin Schutjajew<sup>a</sup>, Erik Troschke<sup>a</sup>, Leonid Kabarov<sup>b,c</sup>,  
Jonas Eichhorn<sup>b,c</sup>, Felix H. Schacher<sup>b,c,d</sup>, Francesco Walenszus<sup>e</sup>, Daniel Werner<sup>f</sup>,  
Martin Oschatz<sup>a,d,\*</sup>

- a. Friedrich-Schiller-University Jena, Institute for Technical Chemistry and Environmental Chemistry, Philosophenweg 7a, 07743 Jena, Germany.
- b. Institute of Organic Chemistry and Macromolecular Chemistry (IOMC), Friedrich Schiller-University Jena, Humboldtstraße 10, D-07743 Jena, Germany.
- c. Jena Center for Soft Matter (JCSM), Friedrich Schiller University Jena, Philosophenweg 7, 07743 Jena, Germany.
- d. Center for Energy and Environmental Chemistry Jena (CEEC Jena), Philosophenweg 7a, 07743 Jena, Germany.
- e. 3P INSTRUMENTS GmbH & Co. KG, Bitterfelder Str. 1-5, 04129 Leipzig, Germany.
- f. Max Planck Institute of Colloids and Interfaces, Department of Colloid Chemistry, Am Mühlenberg 1, 14476 Potsdam, Germany.



**Figure S1.** Transmission electron microscopy (TEM) images of polystyrene spheres.

**Table S1.**  $2\theta$  position of (002) and (100) reflections as well as full width at half maximum (FWHM) from PXRD of hard carbon materials.

	$2\theta$ (002), °	$2\theta$ (100), °	FWHM (002)	FWHM (100)
<b>PS-HC-2</b>	23.55	43.90	5.69	3.81
<b>PS-HC-20</b>	23.92	44.04	5.59	4.19
<b>HC</b>	23.90	44.04	5.99	4.11

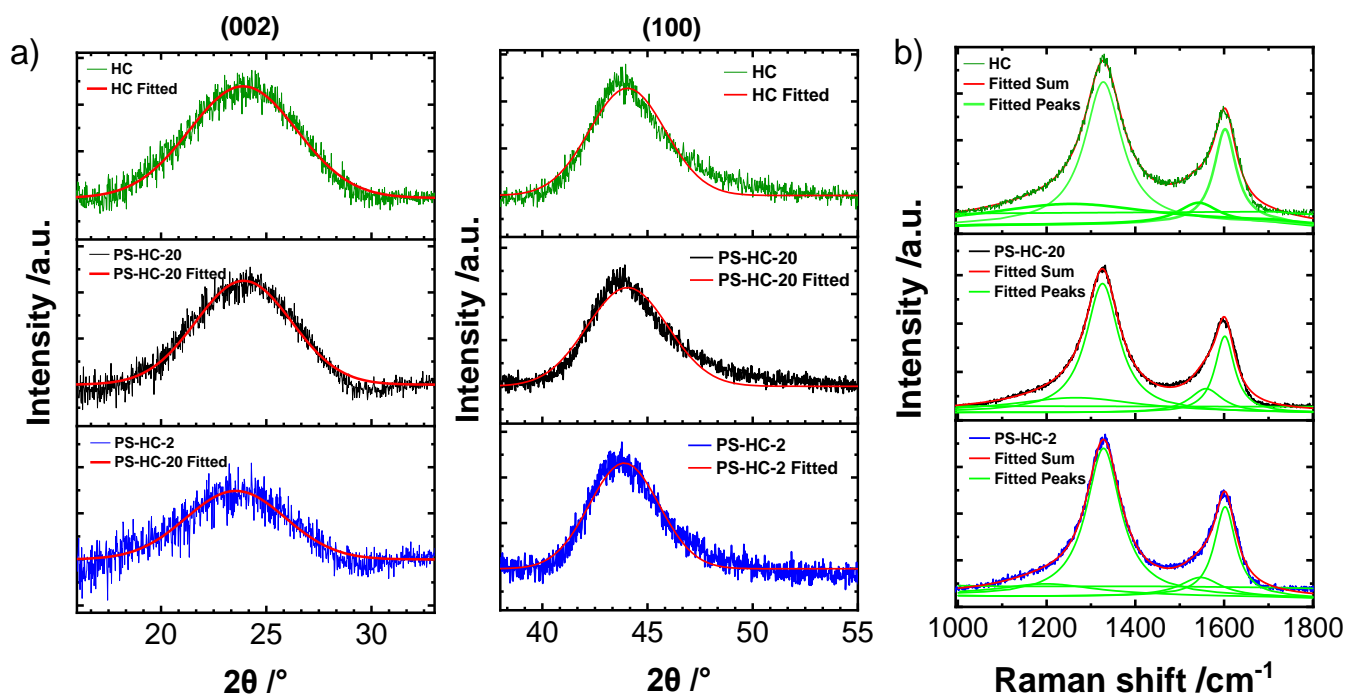


**Figure S2.** Fitted a) (002) and (100) reflections from powder X-Ray diffraction (PXRD) patterns. b) Raman spectra of hard carbon materials.

**Table S2.** Relevant characteristics of a hard carbon crystallite calculated from Scherrer equation.

	The crystalline coherency length in the stacking direction ( $L_c$ ), nm	The size of the layer in the plane direction ( $L_a$ ), nm
PS-HC-2	1.43	2.25
PS-HC-20	1.45	2.04
HC	1.36	2.08

**Table S3.** Intensity ratios of A- and G-band from Raman spectroscopy of hard carbon materials.

	$I_A/I_G$		$I_A/I_G$		$I_A/I_G$
PS-HC-2	0.22	PS-HC-20	0.32	HC	0.22

**Table S4.** Data obtained from physisorption isotherms ( $N_2$  at 77 K and  $CO_2$  at 273 K) of hard carbon materials: QSDFT,  $N_2$  specific surface area and  $N_2$  uptake, 2D-NLDFT,  $CO_2$  pore volume, as well as  $CO_2$  uptake.

	$SSA_{QSDFT,N_2}$ $m^2 g^{-1}$	$N_2$ uptake at 77 K, $cm^3 g^{-1}$	$CO_2$ uptake at 273 K, $cm^3 g^{-1}$	$V_{CO_2(<0.7\text{ nm})}$ , $cm^3 g^{-1}$
PS-HC-2	10	15.1	3.8	0.010
PS-HC-20	1	2.1	0.4	0.003
HC	1	2.0	0.3	0.002

**Table S5.** Elemental analysis data of hard carbon materials.

	C, wt %	O, wt %	H, wt %
PS-HC-2	99.18	0.82	0
PS-HC-20	100.00	0	0
HC	99.93	0.07	0

**Table S6.** Values of  $H_2O$  uptake at 298 K of hard carbon materials.

	$H_2O$ uptake at 298 K, $cm^3 g^{-1}$		$H_2O$ uptake at 298 K, $cm^3 g^{-1}$		$H_2O$ uptake at 298 K, $cm^3 g^{-1}$
PS-HC-2	25.3	PS-HC-20	9.0	HC	12.1

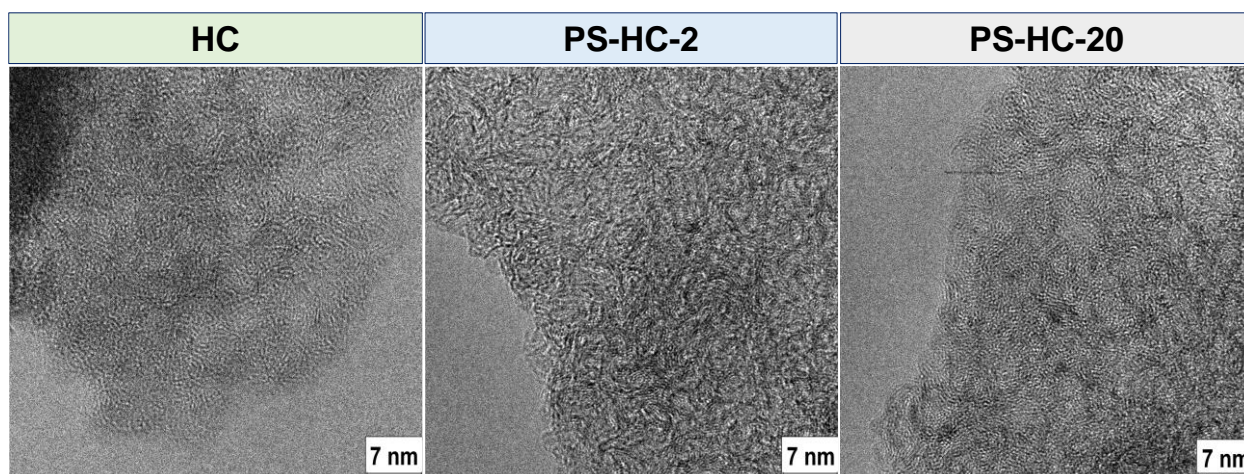


**Figure S3.** TEM images of hard carbon materials.

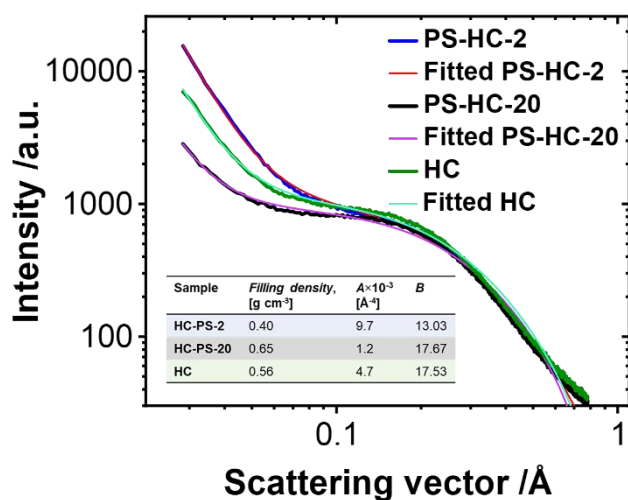


**Figure S4.** Fitted small-angle X-ray scattering (SAXS) curves of hard carbon materials.

**Table S7.** Pore characteristics of the materials determined from N<sub>2</sub> at 77 K and CO<sub>2</sub> at 273 K physisorptions of intermediate carbons after 600°C.

	SSA <sub>QSDFT,N<sub>2</sub></sub> , m <sup>2</sup> g <sup>-1</sup>	V <sub>N<sub>2</sub></sub> , cm <sup>3</sup> g <sup>-1</sup>	V <sub>CO<sub>2</sub>(&lt;0.7 nm)</sub> , cm <sup>3</sup> g <sup>-1</sup>
PS-HC-2-600	566	0.22	0.174
PS-HC-20-600	464	0.20	0.181
HC-600	474	0.18	0.173

**Table S8.** Elemental analysis data of intermediate carbons after 600°C.

	C, wt %	O, wt %	H, wt %
PS-HC-2-600	90.79	6.67	2.54
PS-HC-20-600	90.95	6.75	2.30
HC-600	90.78	6.91	2.31

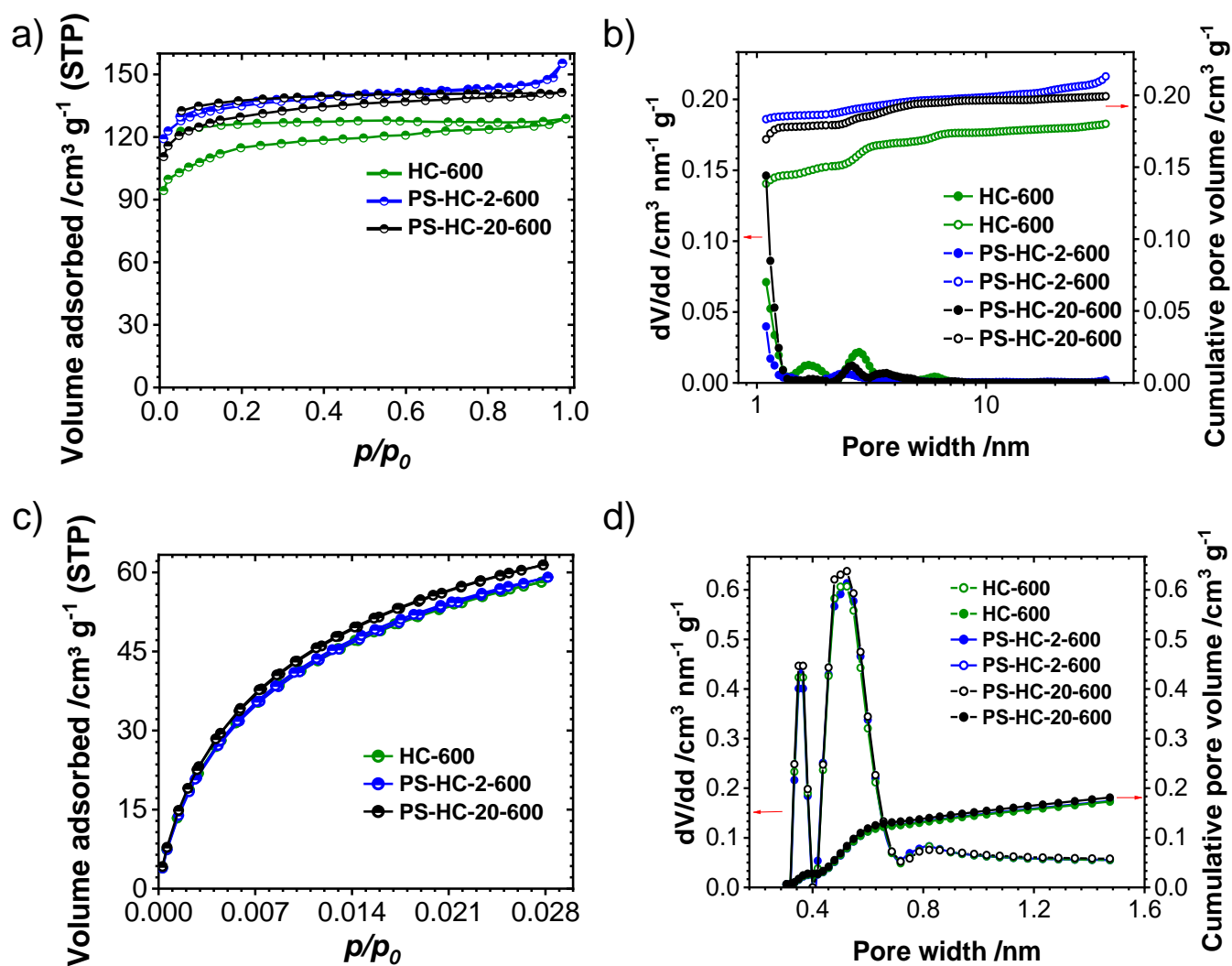


**Figure S5.** a) N<sub>2</sub>-physisorption isotherms at 77 K; c) CO<sub>2</sub>-physisorption isotherms at 273 K; b), d) Calculated pore size distributions of intermediate carbons after 600°C.

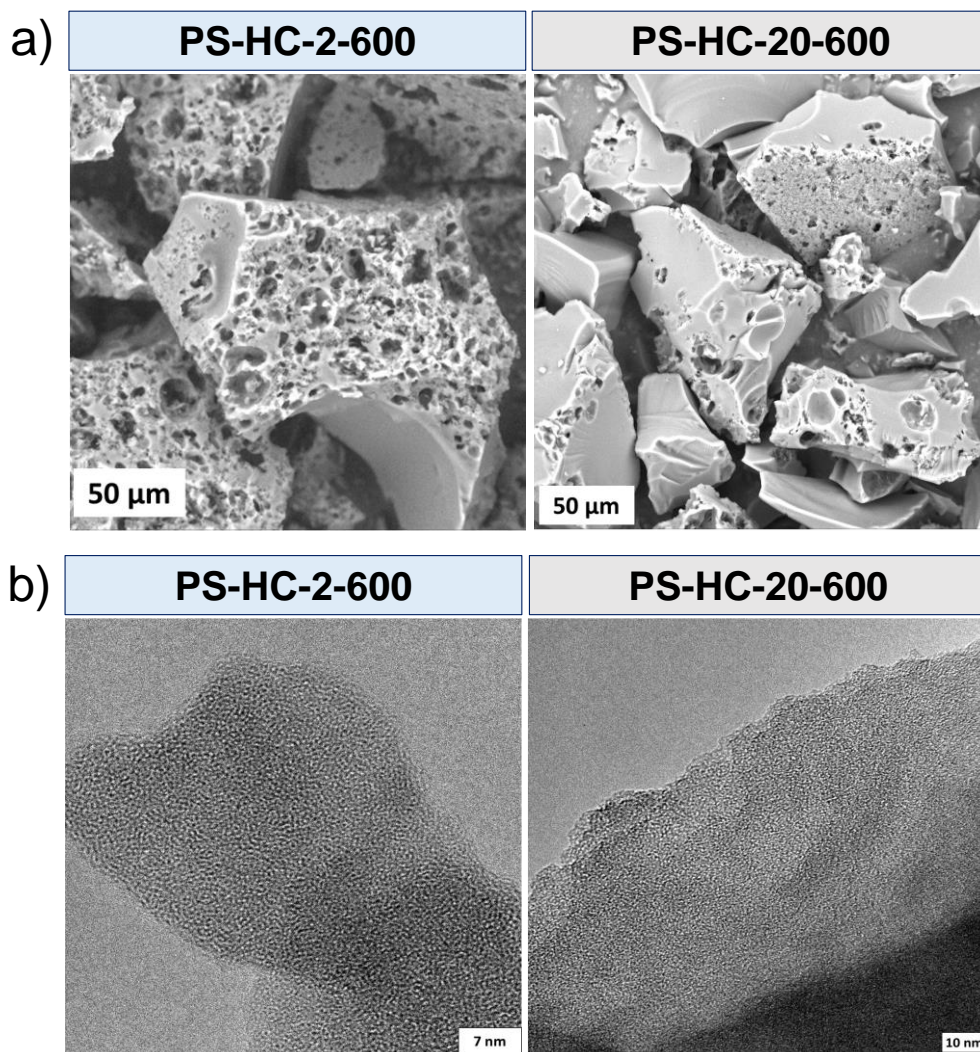


**Figure S6.** a) SEM images. b) TEM images of intermediate carbons after 600 °C.

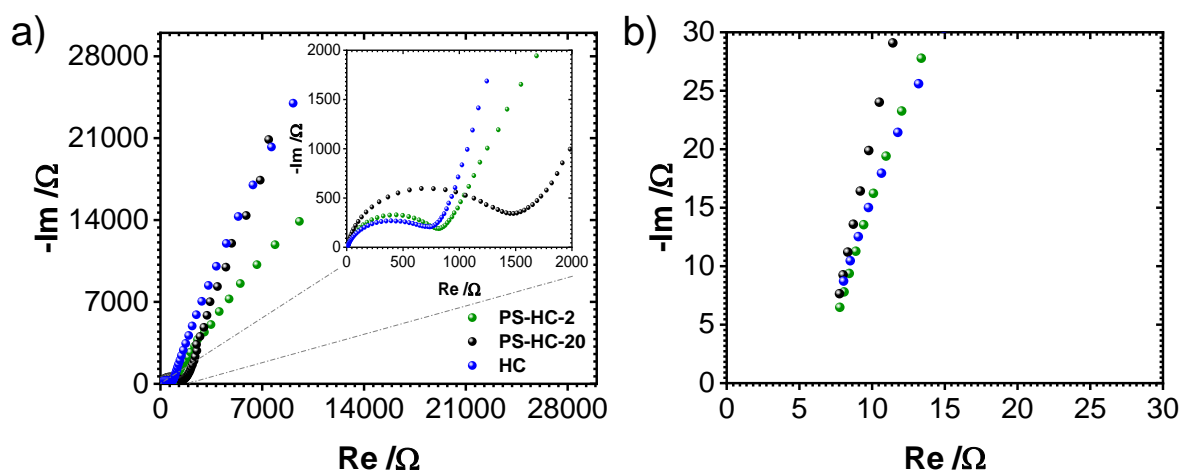


**Figure S7.** Electrochemical impedance spectra of hard carbons unaltered by solid electrolyte interphase (SEI).



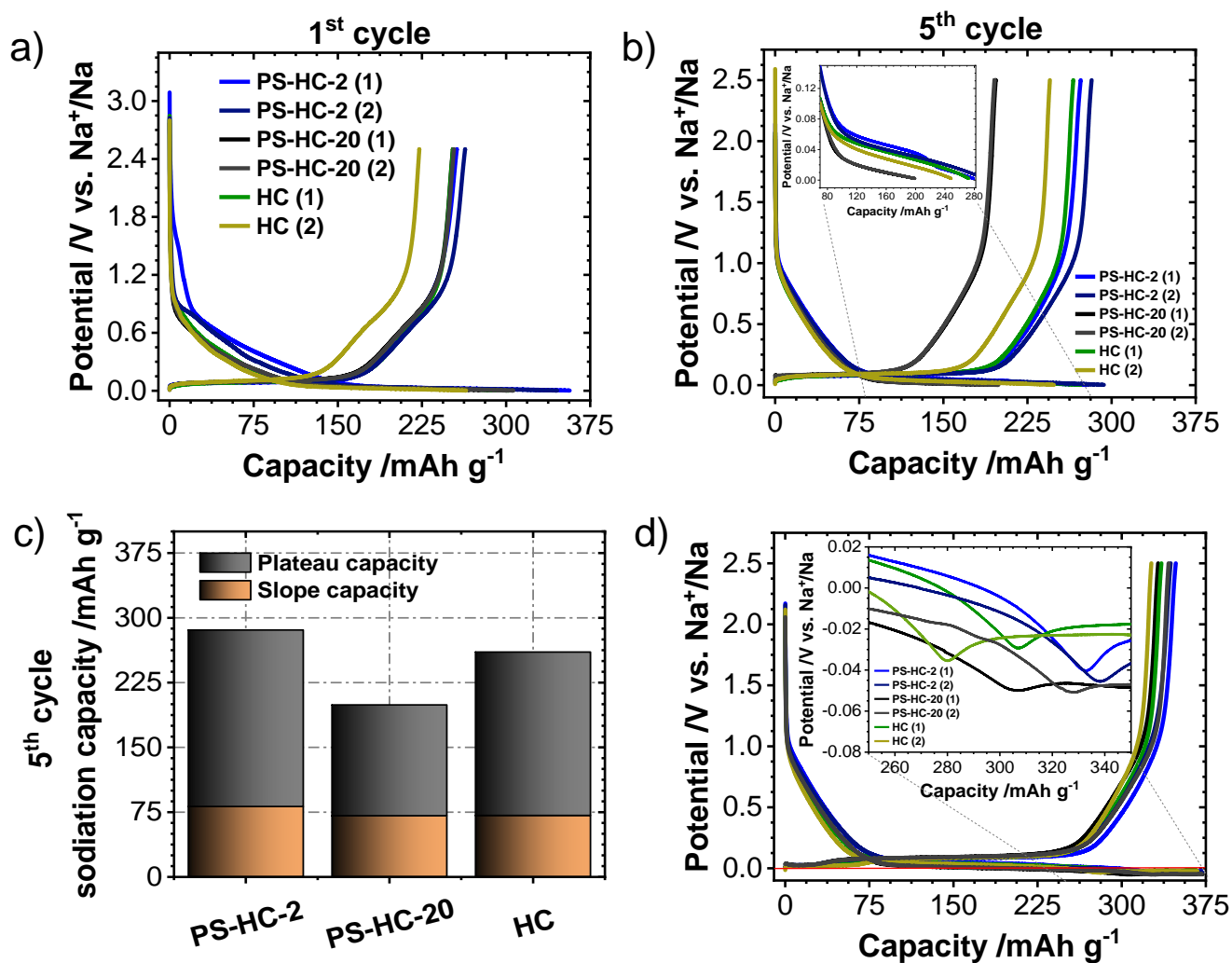


**Figure S8.** Galvanostatic charge-discharge curves of hard carbon materials recorded at C/20 current density from 2 experiments. a) Voltage limited 1<sup>st</sup> cycle. b) Voltage limited stable cycle (5<sup>th</sup>). c) A bar representing average from 2 experiments slope as well as plateau capacities of hard carbon materials in voltage limited stable cycle (5<sup>th</sup>). d) Capacity limited cycle.

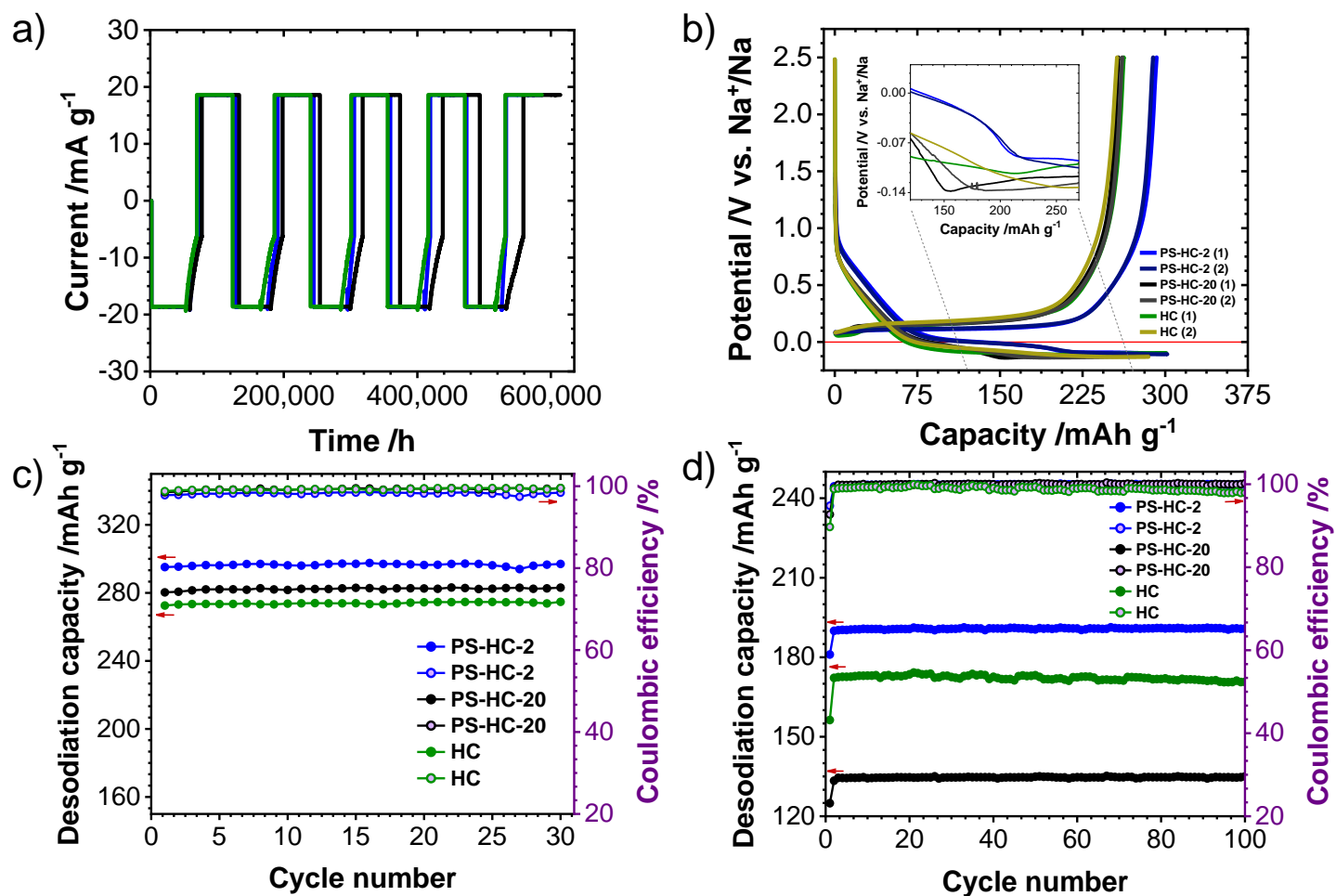


**Figure S9.** a) Representation in the scale current vs time of overall galvanostatic charge-discharge processes at C/20 current density with constant voltage step (2 mV). b) Capacity limited cycle of 2 experiments recorded at C/2 current density. c) Cycling at C/20 current density until 30 cycles with a capacity limitation. d) Cycling at C/2 current density until 100 cycles with a capacity limitation.